Intracellular Trafficking of Hybrid Gene Delivery Vectors

**Rahul K. Keswani**[§,a], **Mihael Lazebnik**[§], and **Daniel W. Pack**[†,*]

[§]Department of Chemical and Biomolecular Engineering, University of Illinois, Urbana, IL 61801, USA

[†]Department of Chemical and Materials Engineering and Department of Pharmaceutical Sciences, University of Kentucky, Lexington, KY 40506, USA

Abstract

Viral and non-viral gene delivery vectors are in development for human gene therapy, but both exhibit disadvantages such as inadequate efficiency, lack of cell-specific targeting or safety concerns. We have recently reported the design of hybrid delivery vectors combining retrovirus-like particles with synthetic polymers or lipids that are efficient, provide sustained gene expression and are more stable compared to native retroviruses. To guide further development of this promising class of gene delivery vectors, we have investigated their mechanisms of intracellular trafficking. Moloney murine leukemia virus-like particles (M-VLPs) were complexed with chitosan (Chi) or liposomes (Lip) comprising DOTAP, DOPE and cholesterol to form the hybrid vectors (Chi/M-VLPs and Lip/M-VLPs, respectively). Transfection efficiency and cellular internalization of the vectors were quantified in the presence of a panel of inhibitors of various endocytic pathways. Intracellular transport and trafficking kinetics of the hybrid vectors were dependent on the synthetic component and used a combination of clathrin- and caveolar-dependent endocytosis and macropinocytosis. Chi/M-VLPs were slower to transfect compared to Lip/M-VLPs due to the delayed detachment of the synthetic component. The synthetic component of hybrid gene delivery vectors plays a significant role in their cellular interactions and processing and is a key parameter for the design of more efficient gene delivery vehicles.

Graphical Abstract
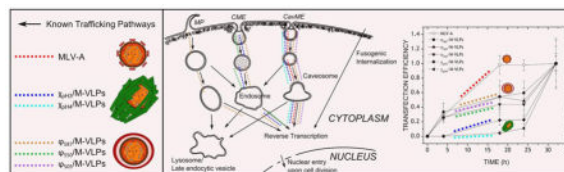
[*]To whom correspondence should be addressed: Phone: 859-218-0907, Fax: 859-257-7585, dan.pack@uky.edu, Department of Chemical and Materials Engineering, Department of Pharmaceutical Sciences, University of Kentucky, 467 Biological Pharmaceutical Building, 789 South Limestone, Lexington, KY 40536-0596, USA.
[a]now at Department of Pharmaceutical Sciences, College of Pharmacy, University of Michigan, Ann Arbor, MI 48109, USA

Keywords

Chitosan; Liposomes; DOTAP; DOPE; Cholesterol; Retrovirus; Hybrid vectors; Gene therapy

INTRODUCTION

Gene therapy promises to be a revolutionary approach for many conditions whereby genetic material is inserted into human cells to provide enhancement or reduction of protein expression for the prevention, treatment or elimination of disease. However, clinical implementation of gene therapy has been difficult. Design of delivery vectors remains a major obstacle to effective gene therapies [1]. In our earlier studies, we reported the design of hybrid synthetic/retroviral vectors using Moloney murine leukemia virus-like particles (M-VLPs) complexed with polymers such as poly-L-lysine (PLL/M-VLP) [2], polyethylenimine (PEI/M-VLP) [2,3] and chitosan (Chi/M-VLP) [4] or liposomes comprising 1,2-dioleyl-3-triammoniumpropane (DOTAP), 1,2-dioleyl-sn-glycero-3-phosphoethanolamine (DOPE) and cholesterol (Lip/M-VLP) [5]. Although these vectors show promise, design of improved hybrid vectors will require an understanding of their delivery mechanisms including cellular internalization and intracellular trafficking.

Gene delivery vectors and other nanoparticles may enter cells via endocytic or non-endocytic pathways [6]. In the absence of chemical or physical manipulation, such as microinjection, electroporation or membrane permeabilization, delivery vehicles may enter cells by fusion with or penetration across the extracellular membrane [7]. Endocytic pathways have long been studied as primary mechanisms of cell entry of nanoparticles including viral and non-viral gene delivery vectors [6,8–11]. Endocytosis occurs through several different mechanisms including macropinocytosis (MP), clathrin-mediated endocytosis (CME) and caveolae-mediated endocytosis (CavME). MP refers to the formation of large irregularly shaped endocytic vesicles called macropinosomes for internalization of extracellular fluid and its contents [2,7,8]. CME is so called due to the formation of clathrin-coated vesicles (CCV) comprising polygonal clusters of clathrin and other adapter proteins enveloping the endocytic vesicle and providing for the internalization of a variety of cellular receptors and their ligands [2,7,9,10]. CavME is a similar receptor-specific internalization pathway, but occurs through vesicles called caveolae, due to their formation by cholesterol-binding proteins known as caveolin, that are rich in cholesterol and glycosphingolipids [6,11,15,16]. Macropinosomes and endosomes follow similar pathways of maturation involving acidification and gain and loss of known endosomal markers prior to fusion with lysosomes, trafficking towards the Golgi complex or exocytosis [12], while caveolae fuse with early endosomes or caveosomes prior to transport to the Golgi complex or endoplasmic reticulum [15]. These vesicles also recycle back to the plasma membrane with the rate of recycling varying between different cells [11].

Chitosan-based gene delivery vectors are internalized via endocytic pathways and driven towards successful transfection through release from endosomes, mainly via the proton-sponge mechanism, due to the presence of excess glucosamines [17]. Lipid-based gene delivery vectors may utilize either endocytotic pathways [18] or membrane fusion [19] for

transfection, mainly dependent on their composition. pH-sensitive lipid molecules like DOPE in liposomal formulations rely heavily on pH-dependent pathways, CME or MP, for endosomal destabilization and release of cargo into the cytosol [17,18]. Cholesterol, when included in the liposomal composition, may be expected to modulate trafficking mechanisms through CavME as it has been associated with caveolin proteins [6,22].

We have investigated the effect of the composition of Chi/M-VLP and Lip/M-VLP on the trafficking mechanisms of hybrid vectors. To elucidate internalization mechanisms, we measured the kinetics of cellular uptake and transfections at 4 °C and 37 °C and in the presence of various pharmacological inhibitors in comparison with murine leukemia viruses containing an amphotropic envelope protein (MLV-A). Furthermore, we visualized the trafficking of the fluorescently-labeled vectors within the cell via confocal fluorescent microscopy.

MATERIALS AND METHODS

Cell Lines and Assays

Human embryonic kidney cells, HEK293 and cervical cancer cells, HeLa were purchased from the American Type Culture Collection (Manassas, VA). The MLV producer cell line, GP293Luc, expressing the MLV viral *gag-pro-pol* genes and a viral packaging sequence encoding neomycin resistance and luciferase reporter genes was purchased from Clontech (Mountain View, CA). All cell lines were grown in DMEM supplemented with 10% FBS (complete media) and cultured at 37 °C in 5% CO_2. Dulbecco's Modified Eagle's Medium (DMEM) and Phosphate-buffered saline (PBS) was produced in-house at the Cell Culture Media Facility, School of Chemical Sciences, University of Illinois. Fetal Bovine Serum (FBS) was bought from Gemini Bio-Products and used as purchased. Luciferase assay and Cell-Titer Blue^{TM} assay kits were bought from Promega and used as per the manufacturer's instructions. BCA assay was bought from Thermo Scientific and used as per the manufacturer's instructions.

M-VLP Production and Quantification

M-VLPs were produced in GP293Luc cells (2×10^6) seeded in a 10 cm dish. The cells were cultured for four days before the M-VLP containing supernatant was collected and filtered through a 0.45 μm surfactant-free cellulose acetate syringe filter. The concentration of M-VLPs in the supernatant was measured using a q-RT-PCR protocol [3]. RNA Standards were obtained from the Clontech qPCR Retroviral Quantification Kit and stored at −80 °C before further use. Viral RNA was extracted using the QIAGEN Viral RNA Extraction kit and stored in a 60 μl eluate at −80 °C before further use. Standards and viral RNA samples were prepared for reverse transcription using Taqman reverse transcription reagents (Applied Biosystems, Carlsbad, CA). Twenty μl samples were mixed in 200 μl PCR tubes using the reagent concentrations suggested by the kit plus 250 nM sequence-specific primers. Thermal cycling was carried out on a Peltier Thermocycler (PTC)-100 (MJ Research). Real-time PCR of the cDNA standards and samples was carried out in triplicate in 10 μl/well samples on a 384-well plate in a Taqman 7900 Real-Time PCR Machine (Applied Biosystems) and analyzed using SDS software (Applied Biosystems). The final

reaction mixture ratio of the components was 5:1:1:3 (2X SYBRGreen real-time PCR reagent:forward primer:reverse primer:cDNA volume). The final concentration of the sample RNA was calculated using the calibration curve obtained via the cDNA standards. Each viral particle has 2 RNA copies which enabled us to calculate the total number of M-VLPs in a given volume of supernatant. Two RNA extracts were collected for each M-VLP sample and quantified using 3 dilutions of each cDNA sample. M-VLP supernatant was either used immediately or stored at 4 °C for short term storage (< 4 weeks) or stored at −80 °C for long term storage.

MLV-A Production

GP293Luc cells, seeded (2×10^6) in a 10 cm dish, were grown for 48 h prior to transfection with the envelope plasmid pMDM.4070A using Lipofectamine® 2000 (LF2000) (Carlsbad, CA, USA). Complete media was replaced with serum-free media just before transfections. Plasmid:LF2000 vectors were synthesized in the required stoichiometric ratios and incubated at room temperature for 10 min prior to drop-wise addition to GP293Luc cells. The media was replaced again with complete media 6 h post-transfection. The cells were cultured for a further 48 h before the MLV-A containing supernatant was collected and filtered through a 0.45 µm surfactant-free cellulose acetate syringe filter. Viral titer was quantified via the RT-PCR assay as described above.

Synthesis of Lip/M-VLP

Hybrid vectors were synthesized as published before [5]. In brief, the three lipids dissolved in chloroform (Avanti® Polar Lipids) were mixed in the desired composition in a test-tube and dried under vacuum overnight to form a thin film. The lipid film was rehydrated using a 5% glucose solution and sonicated briefly to allow the lipids to dissolve completely. The rehydrated solution was vortexed every 30 minutes for 30 seconds for a total duration of 3 h. If not used immediately, the lipid solution was stored at 4 °C (< 1 month). The lipid solution was extruded through an Avanti® Mini-Extruder for 11 passes through a 100 nm PC membrane. The lipid samples were then added to the required volume of M-VLP supernatant and diluted in 5% glucose solution as per the Lip/M-VLP stoichiometry and incubated for 2 h at 4 °C prior to further analysis or transfection.

Synthesis of Chi/M-VLP

Hybrid vectors were synthesized as published before [4]. Chitosan (Molecular Weight = 190–310 kDa, Sigma Aldrich, 1 mg/ml dissolved overnight at 55 °C in 0.6 % acetic acid and filtered through a 0.22 µm surfactant-free cellulose acetate syringe filter, pH 3 and 4) was added drop-wise to required volume of M-VLP supernatant while vortexing to achieve the desired polymer:M-VLP ratio. The hybrid vectors were then incubated at 4 °C for 4 h.

Drug Cytotoxicity and Compatibility Studies

The toxicity of drugs was determined using the Cell Titer-Blue™ Cell Viability Assay. HEK293 cells were seeded in a 96-well plate at 5×10^4 cells/well 18–24 h prior to addition of drugs. Different concentrations of drugs were added to the cells in serum-free medium and left for 5 h before the medium was replaced with complete media. Fifteen µl of Cell

Titer-Blue[TM] reagent was added to each well 24 h after the addition of drugs. The cells were incubated for further 4 h at 37 °C before adding 100 µl per well of stop reagent following which fluorescence (λ = 570 nm, 650 nm) was measured in a SpectraMax 340PC 96-well plate reader. For compatibility studies, HEK293 cells permanently expressing luciferase (HEK293Luc) were seeded at 4×10^5 cells/well in a 12-well tissue culture plate 18–24 h prior to addition of drugs. Different concentrations of drugs (up to the highest concentration with minimal toxicity) were added to the cells in serum-free medium and left for 5 h before the medium was replaced. Luciferase expression was measured 48 h post addition of drugs as mentioned above.

Transfections

HEK293 cells were seeded 18–24 h prior to transfection at 4×10^5 cells/well in 12 well plates. Growth media containing serum was replaced with serum-free DMEM prior to drop-wise addition of vectors and replaced again with normal growth media 4 h post-transfection. For serum studies, the transfection media contained 0–50% serum. For temperature-dependent transfection experiments, cells were maintained at 4 °C or 37 °C for 4 h following which media was replaced again with complete media. For transfections with MLV-A, HEK293 cells were seeded 18–24 h prior to transfection at 8×10^4 cells/well in 6-well plates. MLV-A containing supernatant was diluted in complete media (1:1 or 1:3, v:v) along with addition of 1 µl Sequabrene for every 1 ml of the diluted mixture to produce viral media. HEK293 cells were transfected with 1 ml/well viral media.

Luciferase expression assay

Luciferase expression was quantified at required time-points using the Promega luciferase assay system following the manufacturer's protocol. Luciferase activity was measured in relative light units (RLU) using a Lumat LB 9507 luminometer (Berthold, GmbH, Germany). Lysate protein concentration was then determined by BCA assay to standardize expression values.

Fluorescent Labeling of Hybrid Vectors

20 ml of M-VLP supernatant was centrifuged at 60,000g for 2 h at 4 °C and the pellet was resuspended in 50 mM HEPES with 145 mM NaCl at a density of 1×10^{10} M-VLPs/ml. 1,1′-dioctadecyl-3,3,3′,3′-tetramethylindodicarbocyan-ine, 4-chlorobenzenesulfonate salt (DiD) (Invitrogen, 1 mM in DMSO, Ex = 644 nm, Em = 665 nm) was added to the resuspended M-VLPs to give a final concentration of 2 µM DiD. The mixture was incubated for 1 h at room temperature. Labeled M-VLPs were separated from the free dye through a PD-10 gel filtration desalting column (GE Healthcare). Labeling of chitosan with Rhodamine-B Isothiocyanate (RITC) was performed as described before [23,24]. In brief, 10 ml of chitosan (Molecular Weight = 190–310 kDa, Sigma Aldrich) was prepared at 10 mg/ml dissolved overnight at 55 °C in 0.6 % acid and filtered through a 0.22 µm surfactant-free cellulose acetate syringe filter, pH 3 and 4). An equal volume of methanol as the chitosan solution was then added under stirring. After 3 h, the solution was degassed and kept under N_2 atmosphere. Rhodamine-B isothiocyanate was dissolved in methanol at a concentration of 4 mM and 2.64 mL was injected into the chitosan solution under stirring. The reaction mixture was protected from light and left to proceed for 17 hours. The

unreacted rhodamine B-isothiocyanate was removed by precipitation of chitosan with drop-wise addition of 0.2 M NaOH to the mixture until the pH is above 10. After 5 washes with deionized water and centrifugations (3500 rpm, 5 min), the chitosan precipitate was recovered for freeze-drying. The chitosan-RITC pellet was resuspended in 0.6 % acid at pH 3 and pH 4. For fluorescently labeled Chi/M-VLP, chitosan-RITC was added drop-wise to required volume of fluorescently labeled M-VLP while vortexing as per the desired stoichiometry. The hybrid vectors were then incubated at 4 °C for 4 h. Fluorescently labeled Lip/M-VLP were generated in a similar fashion as Lip/M-VLP except that DOPE-Rhodamine-B and NBD-6 cholesterol were included in the lipid formulation up to 3% of the total DOPE and Cholesterol content in the vector.

Uptake Studies

Hybrid vectors with fluorescently labeled M-VLPs were synthesized as described above. HEK293 cells were seeded in 12-well plates at 4×10^5 cells per well 18–24 h prior to transfection. Growth media containing serum was replaced with serum-free DMEM 1 h prior to drop-wise addition of vectors. For temperature-dependent uptake experiments, cells were maintained at 4 °C or 37 °C for 4 h following which media was replaced again with complete media. The target cells were washed with PBS containing 0.001% SDS at 2, 4 and 8 h post transfection to remove surface-bound, uninternalized vectors followed by a regular PBS wash. Cells were then trypsinized followed by neutralization with 50 μl of FBS, collected, and analyzed by flow cytometry (10,000 cells) using a Becton Dickinson (Franklin Lakes, NJ) LSR II Flow Cytometer with a 633 nm laser.

Drug Inhibitors-based Trafficking Studies (Transfections)

Hybrid vectors were synthesized as stated above. HEK293 cells were seeded 18–24 h prior to transfection at 4×10^5 cells/well in 12-well plates. Growth media containing serum was replaced with serum-free DMEM along with addition of predetermined concentrations of drugs. After 1 h of incubation with drugs, hybrid vectors were added drop-wise. The transfection media was replaced again with complete media 4 h post-transfection. Luciferase expression was measured 48 h post transfection as mentioned above.

Drug Inhibitors-based Trafficking Studies (Uptake)

Hybrid vectors with fluorescently labeled M-VLPs were synthesized as described above. HEK293 cells were seeded in 12-well plates at 4×10^5 cells per well 18–24 h prior to transfection. Growth media containing serum was replaced with serum-free DMEM along with addition of predetermined concentrations of drugs. After 1 h of incubation with drugs, hybrid vectors were added drop-wise. The target cells were washed with PBS containing 0.001% SDS 2 h post transfection to remove surface-bound, uninternalized vectors followed by a PBS wash. Cells were then trypsinized followed by neutralization with 50 μl of FBS, collected, and analyzed by flow cytometry (10,000 cells) using a Becton Dickinson (Franklin Lakes, NJ) LSR II Flow Cytometer with a 633 nm laser.

Confocal Microscopy

HEK293 cells were seeded at 4×10^5 cells per well of a 6-well plate on a cover slip 46 h prior to transfections. The cells were then transfected with fluorescently labeled Lip/M-VLP and Chi/M-VLP synthesized as described before. Slides of the transfected cells were prepared at 4, 8 and 20 h post-transfection as follows. The cells were washed twice with 1 ml PBS, fixed with 1 ml 3.7% formaldehyde solution and incubated at room temperature in the dark for 20 mins. The cells were washed again with 1 ml PBS. A drop of mounting solution (ProLong® Gold Antifade Reagent with DAPI, Life Technologies, Carlsbad, CA, USA) was placed on a glass slide. The cover slip was wedged out with a forceps and placed face-down onto the glass slide directly over the drop of mounting solution. The four edges of the cover slip were then sealed with clear nail polish and kept at 4 °C. The glass slides were then visualized with a Zeiss LSM 700 Confocal Microscope using the optimal excitation (λ) wavelengths – DiD (λ=633 nm), Rhodamine-B (λ = 555 nm), NBD-6 cholesterol (λ = 488 nm), DAPI (λ = 405 nm). The data was then visualized in Imaris (Bitplane AG, Zurich, Switzerland)

Reverse Transcription Inhibition

Hybrid vectors were synthesized as stated above. HEK293 cells were seeded 18–24 h prior to transfection at 4×10^5 cells/well in 12-well plates. Growth media containing serum was replaced with serum-free DMEM followed by drop-wise addition of hybrid vectors. The transfection media was replaced again with complete media 4 h post-transfection. Azidothymidine (AZT) was added to the transfected cells at 0, 4, 18, 24 and 32 h post-transfection at predetermined concentrations. Luciferase expression was measured 48 h post transfection as mentioned above.

Statistical Analysis

All statistical analyses mentioned in this study was done using the Student's t-test. A result was deemed not significant if $p > 0.05$. (# - $p < 0.05$; ## - $p < 0.02$; ### - $p < 0.002$; * - $p < 0.0002$).

RESULTS

We have previously reported that Chi/M-VLP formed using chitosan at pH 3 (Chi$_{pH3}$/M-VLP) are more efficient than Chi/M-VLP formed with higher pH chitosan solutions (e.g., Chi$_{pH4}$/M-VLP) [4]. Similarly, Lip/M-VLP efficiency depends on the lipid composition with DOTAP:DOPE:cholesterol 5:8:7 w:w:w (Lip$_{587}$/M-VLP) being the most efficient [5]. Here, we have included several of the non-optimal compositions, Chi$_{pH4}$/M-VLP, Lip$_{505}$/M-VLP and Lip$_{550}$/M-VLP, to further understand how the non-viral composition affects hybrid vector efficiency.

Effect of Time and Temperature on Cellular Uptake and Transfection Efficiency of Chi/M-VLP and Lip/M-VLP

Endocytosis is an active, energy-dependent process whereby the vectors use the cell machinery to gain entry through vesicles and are directed towards the appropriate intracellular location. Alternatively, fusogenic internalization is a non-specific mechanism

wherein the vectors enter the cell through passive fusion with the plasma membrane. Endocytosis being an energy dependent process is inhibited at lower temperatures (4 °C) while the fusion mechanism is minimally affected by temperature [6].

In order to determine if hybrid vectors are internalized via endocytosis or fusion mechanisms, we transfected HEK293 cells with Chi/M-VLP or Lip/M-VLP in serum-free media at 4 °C or 37 °C and assayed for luciferase expression at regular intervals up to 48 h after transfection. Chi/M-VLP displayed significantly lower transfection efficiency at 4 °C compared to 37 C (Figure 1a–d). Transfection efficiency of Lip/M-VLP was even more severely reduced at 4 °C compared to 37 °C (Figure 2a–c). Similarly, MLV-A transduction suffered severe reduction at 4 °C compared to 37 °C (to 17%, Figure S1).

In order to investigate if the low transfection efficiency at 4 °C was due to reduced cellular uptake, we repeated the experiment with M-VLP fluorescently labeled with DiD and measured cell-associated fluorescence via flow cytometry at 2, 4 and 8 h post-transfection. Cellular uptake of Chi/M-VLP was higher in HEK293 cells transfected at 37 °C than at 4 °C. Minimal internalization was observed during incubation at 4 C (2 and 4 h) but increased upon the change in incubation temperature from 4 °C to 37 °C at 4 h post transfection (Figure 1e–h). This implied that the vectors attached to the plasma membrane were unable to enter the cells via fusion but were actively endocytosed at a higher temperature.

In contrast, cellular uptake of Lip/M-VLP at 4 °C was similar to 37 °C especially for Lip_{587}/M-VLP (Figure 2d–f) but the transfection followed a similar pattern as Chi/M-VLP (Figure 2a–c). Uptake further increased for Lip_{587}/M-VLP in HEK293 cells after change in incubation temperature to 37 °C. Cellular uptake of Lip_{505}/M-VLP and Lip_{550}/M-VLP was also significantly high at 4 °C (~40% and ~50% compared to uptake at 37 °C, respectively) in the first 4 h. Uptake marginally improved after replacement of media and increase in the incubation temperature.

Effect of Pharmacological Inhibitors on Cellular Uptake and Transfection Efficiency of Chi/M-VLP and Lip/M-VLP

Pharmacological inhibitors are often used to study intracellular trafficking mechanisms of drug and gene delivery vectors [6] (Table 1). These inhibitors are also typically toxic beyond certain concentrations and could potentially inhibit the transgene expression via non-specific mechanisms [25]. Thus, inhibitor concentrations were optimized for both toxicity in HEK293 cells and their effect on luciferase expression in HEK293Luc cells (HEK293 cells permanently expressing luciferase) (Figure S2). The highest drug concentration that resulted in > 90% cell viability in HEK293 cells and minimal effect on luciferase expression in HEK293Luc cells was chosen for further study. Table 1 summarizes both the concentrations used for this study as well as the pathways affected through the use of each drug.

HEK293 cells were transfected with MLV-A in the presence of inhibitors as a control for comparing the changes in the trafficking mechanisms due to the presence of the synthetic component in place of the amphotropic envelope protein. MLV-A transfection decreased significantly in the presence of both CCN (to 37%, $p < 0.02$) and GST (to 59%, $p < 0.05$) (Figure 3a) but was unaffected by the other drugs in the study. This implied that MLV-A

internalized via CavME leading to successful transfection, which is consistent with previous reports of MLV-A transduction mechanisms [37,38].

Uptake of Chi_{pH3}/M-VLP was significantly affected when CavME (to 47% with GST, $p <$ 0.002) [4] or MP (to 73% with AMD, $p < 0.05$) (Figure 3c) was inhibited and transfection efficiency was severely reduced when CavME was inhibited (to 9% with GST, $p < 0.002$) or when actin microfilaments were disrupted (to < 1% with CCN, $p < 0.002$) (Figure 3a). There was also a reduction in transfections when endosomal acidification (to 29% with BFN, $p < 0.02$) [4] or early-stage CME (to 57% with CPZ, $p < 0.05$) was inhibited. CME and CavME were both significantly responsible for successful gene delivery. Since it appears that membrane fusion of Chi_{pH3}/M-VLP was not important for uptake (Figure 1a–d, e–h), the significant reduction in transfection efficiency due to actin disruption can be attributed to the disruption of CavME by CCN.

Uptake of Chi_{pH4}/M-VLP was promoted when CME was inhibited (to 238% with AMN, $p < 0.02$) due to stabilization of clathrin-coated vesicles (CCV) and when actin microfilaments were disrupted (to 141% with CCN, $p < 0.05$) (Figure 3c). However, transfections were severely hampered due to inhibition of CME when CCV formation was inhibited (to 4% with CPZ, $p < 0.0001$), or MP was disturbed (to 48% with AMD, $p < 0.002$ or to 0% with CCN, $p < 0.0001$) and even when caveolar trafficking was hampered (to 14% with GST, $p < 0.002$) (Figure 3a). However, in comparison to Chi_{pH3}/M-VLP, there was no significant effect of BFN on transfection or uptake of Chi_{pH4}/M-VLP.

Cellular uptake of Lip_{505}/M-VLP decreased in the presence of CME inhibitor CPZ (to 73%, $p < 0.05$) or CavME inhibitor GST (to 40%, $p < 0.0001$) (Figure 3d) while transfection efficiency decreased when CME was affected (to 43% with AMN, $p < 0.02$; to 18% with CPZ, $p < 0.002$). Furthermore, transfections were severely reduced when CavME was inhibited (to 4% with GST, $p < 0.0001$) and when actin filaments were disrupted (to 5% with CCN, $p < 0.0001$) (Figure 3b).

For Lip_{550}/M-VLP, cellular uptake increased with caveolar inhibition (to 135% with GST, $p < 0.05$) (Figure 3d). Transfection efficiency increased when MP was affected (to 131% with AMD, $p < 0.02$) but decreased with CME inhibition (to 20% with CPZ, $p < 0.0001$) (Figure 3b). Also, transfections were hampered with CavME inhibition (to 6% with GST, $p < 0.0001$) and when actin polymerization was affected (to 22% with CCN, $p < 0.0001$) (Figure 3b). Importantly, transfections were also reduced when the endosomal V-ATPase machinery was inhibited (to 57% with BFN, $p < 0.02$).

Interestingly, cellular uptake of Lip_{587}/M-VLP was unaffected in the presence of any of the inhibitors (Figure 3d) while transfection efficiency decreased when CME was inhibited (to 35% with CPZ, $p < 0.02$) and MP was inhibited (to 47% with AMD, $p < 0.02$). Transfections were also severely reduced when caveolar trafficking was affected (to 4% with GST, $p < 0.0001$) and actin polymerization was affected (to 9%, $p < 0.0001$) (Figure 3b).

Effect of Serum Proteins on Transfection Efficiency

The presence of serum in transfection media is known to inhibit transfections by many gene delivery vectors, particularly for positively charged species which can interact with serum proteins [39–44]. Furthermore, undesired interactions with serum *in vivo* (50% (v:v) of blood [45]) may decrease vector activity or increase their clearance from the body before providing the desired therapeutic effect. It is critical for gene delivery vectors to resist these non-specific interactions with serum in order to be efficacious for *in vivo* gene delivery. We tested our hybrid vectors in comparison with MLV-A in the presence of serum (up to 50% v:v) in transfection media. Chi/M-VLPs at three different stoichiometries of 4, 7 and 10 $\mu g/10^9$ M-VLPs were able to maintain their efficiency in the presence of up to 20% serum, but the efficiency decreased to 10–20% in 50% serum (Figure 4a). MLV-A exhibited a similar trend with transfections decreasing to 40% in the presence of 50% serum. Transfection by Lip/M-VLPs, however, was completely inhibited in the presence of 10% serum (Figure 4b) irrespective of the composition of the lipids. It has been reported that the inclusion of cholesterol in cationic lipid formulation leads to better serum resistance [39]. However, no significant change was measured in serum resistance between Lip_{587}/M-VLPs and Lip_{505}/M-VLPs.

Measurement of Trafficking Kinetics via Inhibition of Reverse Transcription of MLV-A, Chi/M-VLP and Lip/M-VLP

AZT is a potent inhibitor of reverse transcriptase and was one of the first anti-retroviral drugs approved for the control of HIV [36]. The addition of AZT to the transfection media is expected to block the transfection of MLV-A and the hybrid vectors at the last trafficking step prior to nuclear entry, i.e. by preventing the formation of the provirus. When added to cells during the transfection period, AZT blocks all further reverse transcription, effectively disallowing any further transfection while vectors that had been reverse transcribed prior to the addition of AZT go on to integrate and express the luciferase gene. Thus, the use of AZT served as an effective method to measure trafficking kinetics of vectors prior to nuclear entry.

MLV-A transfection was quicker than any of the hybrid vectors. The transfection efficiency was unchanged when AZT was added at 16, 24 and 32 h post-transfection (Figure 5). This implied that MLV-A had undergone reverse transcription by 16 h. In contrast, addition of AZT at 32 h post-transfection with the hybrid vectors led to a significant increase in transfections compared to AZT addition at 24 h. In addition, Chi/M-VLP were much slower than Lip/M-VLP, with Chi/M-VLP having reached < 25% efficiency at the 24 h time point compared to 32 h whereas Lip/M-VLP had reached 45–60% at the same time-points (Figure 5).

Visualization of trafficking of Chi/M-VLP and Lip/M-VLP through confocal microscopy

In order to confirm the kinetics of hybrid vector transfections as measured via AZT inhibition studies, we used confocal microscopy to visualize fluorescently labeled vectors at three time-points: 4 h, 8 h and 20 h post-transfection. M-VLPs were labeled with the lipophilic dye DiD. Chitosan was labeled with rhodamine-B isothiocyanate using a previously reported protocol [22,23]. For visualizing Lip/M-VLP, DOPE labeled with

rhodamine-B (DOPE-Rhod-B) and NBD-6 cholesterol were added to the lipid formulation. Lip/M-VLP was supplemented with DOPE-Rhod-B up to 3% of total DOPE content and with NBD-6-chol up to 3% of total cholesterol content.

The colocalization of chitosan and M-VLPs was maintained even at 20 h post-transfection implying that Chi/M-VLP remained complexed for at least 20 h (Figure 6a, Figure S3) and was most likely a reason for the slower trafficking kinetics of Chi/M-VLP (Figure 5). In contrast, while colocalization was observed for Lip/M-VLP at 4 h (Figures S3–S5), a rapid decay in the fluorescence signal of DOPE-Rhod-B and NBD-6-chol was observed along with significant loss of colocalization between M-VLP and the fluorescent lipids at 8 h and 20 h. (Figure 6b, Figures S4–S5). This supports the trend observed in the transfections in presence of AZT (Figure 5) that more rapid trafficking of Lip/M-VLP compared to Chi/M-VLP was due to the separation of the synthetic lipids from M-VLPs occurring earlier than chitosan.

DISCUSSION

Hybrid vectors bridge the gap between synthetic and viral vectors and are novel design innovations for development of gene therapy vectors. In our hybrid vectors, M-VLPs lack the envelope protein without which cellular uptake is impossible. Hence, successful transfection requires the synthetic component to initiate interaction with the cell and mediate internalization.

Both Chi/M-VLP and Lip/M-VLP have positively charged synthetic components that associate with unknown components of the negatively charged cell membrane. In contrast, the amphotropic envelope protein of MLV-A interacts with the Pit2 receptor on HEK293 cells leading to caveolar uptake [37]. The composition of liposomes consisting of DOTAP, DOPE and cholesterol significantly affects the different endocytic mechanisms involved in cellular uptake as well as trafficking pathways within the cell. For example, DOPE promotes liposomal-endosomal fusion (CME) through conversion to a hexagonal inverted phase (H_{II}) thereby allowing escape of the vectors into the cytosol [9,46]. On the other hand, cholesterol primarily associates with other cholesterol-rich moieties within the cell (CavME) [9,45]. Chitosan has been implicated in multiple trafficking routes dependent on the cell type and cargo [47–49]. Our recent reports have shown that Chi_{pH3}/M-VLP [4] and Lip_{587}/M-VLP [5] are optimal in terms of transfection efficiency and morphology. Herein, we elucidate the mechanisms of their trafficking and gene delivery efficiency in relation to other sub-optimal hybrid vectors, Chi_{pH4}/M-VLP, Lip_{505}/M-VLP and Lip_{550}/M-VLP.

Measurement of transfection efficiency and cellular uptake at low (4 °C) and high (37 °C) temperature made it possible to distinguish between endocytosis (active only at 37 °C) and fusogenic mechanisms (temperature independent) for cellular uptake. We found that MLV-A, Chi/M-VLP and Lip/M-VLP primarily relied on endocytic mechanisms for successful transfections (Figure 1a–h). Lip/M-VLP were also able to fuse with the plasma membrane as shown by internalization at 4 °C but were unsuccessful in transfection via this route (Figure 2a–f). These results are consistent with recent reports [50] that have discredited plasma membrane fusion as a mechanism in successful liposomal gene delivery [19].

Uptake of Chi/M-VLP increased significantly between 4 and 8 h post-transfection (Figure 1e–h). In contrast, during Lip/M-VLP transfection, cellular fluorescence remained constant or marginally decreased between 4 and 8 h (Figure 2d–f). This suggested that loss of the M-VLP lipid bilayer, which contains the lipophilic DiD dye, was already being initiated within 4–8 h post-transfection. DiD is fluorescent only upon being in a lipophilic environment. Upon removal of the lipid bilayer, it is likely that the dye was diluted into cellular membranes and potentially eliminated from the cell, leading to a decrease in fluorescence.

MLV-A transduction relied on CavME as indicated by the reduction in the presence of GST (Figure 3a). While the role of actin in MLV-A trafficking is uncertain, it is known that actin depolymerization by CCN leads to reduced caveolae formation without disrupting clathrin-dependent uptake, thus leading to reduced transfections in the presence of CCN [34]. Indeed, it is known that MLV-A trafficking is caveolae dependent utilizing the Pit2 receptor for efficient uptake [37].

The reduction of Chi_{pH3}/M-VLP transfection in the presence of BFN suggested these vectors were able to use CME for effective transfections, whereas Chi_{pH4}/M-VLP were unable to involve CME in their trafficking (Figure 3a,c) [4] relying heavily on CavME. Hence, it appears that varying the chitosan stock pH used to synthesize the vectors resulted in modified trafficking pathways, likely due to the differing size of the vectors [4]. In addition, it can be inferred that CME is a highly effective intracellular trafficking mechanism for Chi/M-VLP since Chi_{pH3}/M-VLP that used CME had a higher transfection efficiency compared to Chi_{pH4}/M-VLP that used only CavME towards successful gene delivery [4] (Figure 3a,c). Therefore, not only does chitosan pH play a significant role in Chi/M-VLP morphology, it also optimizes trafficking for efficient transfection of Chi/M-VLP.

Transfection efficiencies of Chi/M-VLP increased 5- to 20-fold between 18 and 24 h post-transfection, while Lip_{587}/M-VLP transfections increased 1.5-fold over the same time period (Lip_{505}/M-VLP and Lip_{550}/M-VLP were nearly constant). In addition, 23% of Chi_{pH3}/M-VLP versus 60% of Lip_{587}/M-VLP had undergone reverse transcription by 24 h (Figure 5) compared to at 32 h. Finally, confocal fluorescence microscopy revealed a higher degree of colocalization of chitosan with M-VLPs compared to liposomes (Figure 6, Figure S3). These data suggest that the trafficking of Chi/M-VLP was slower than that of Lip/M-VLP due to delayed release of the chitosan synthetic envelope. Additionally, the composition of the synthetic lipids did not have a significant impact on the trafficking kinetics from 0 – 32 h (Figure 5). MLV-A was the fastest amongst all our vectors because the hybrid vectors had an additional barrier in delivery, namely, the stripping of the synthetic component.

Given the quick removal of the synthetic lipids (Figure 5, Figure 6b, Figures S3–S5), it may be surprising that the lipids were able to exert a significant influence on the trafficking process of M-VLPs despite being a component of the hybrid vector for a shorter duration than Chi/M-VLP. For Lip_{505}/M-VLP, CavME played a significant role in the trafficking pathway (Figure 3b,d) as expected given the cholesterol heavy composition of the synthetic lipids. The transfection efficiency for Lip_{550}/M-VLP was affected when CME was inhibited and promoted when MP was inhibited (Figure 3b,d). Thus, CME was a significant pathway

for Lip_{550}/M-VLP while CavME played a small role in the late-stage trafficking possibly through interplay between the late-stage endosomes and caveosomes [51]. Since all three lipids were present in the Lip_{587}/M-VLP, it is possible that both the neutral helper lipids helped to promote a preferred pathway (DOPE for CME and cholesterol for CavME). Cellular uptake was not significantly affected in the presence of any drugs since other pathways were a viable option for Lip_{587}/M-VLP as compensatory mechanisms.

It is evident that the inclusion of DOPE and cholesterol as neutral-helper lipids in Lip/M-VLP was critical for highly efficient gene delivery. The presence of DOTAP alone provided much higher uptake of M-VLPs compared to other liposomal formulations but failed at efficient gene delivery [5]. Moreover, our results here suggest that DOPE and cholesterol were able to interact with the cellular machinery to achieve the high transfection efficiency reported previously [5].

Interaction of gene delivery vectors with serum proteins often leads to reduced performance *in vivo* through binding of negatively-charged serum components with the positively charged complexes leading to reduced uptake, structural re-organization of the complex, colloidal instabilities and increased clearance by the reticuloendothelial system (RES) [43,44]. In our serum-interaction experiments, the vectors were present in the transfection media containing 0–50% serum for 4 h prior to being replaced by complete media (with 10% serum) (Figure 4). While M-VLPs and MLV-A have a very low negative surface charge, Chi/M-VLP and Lip/M-VLP have a high positive surface charge [4,5] leading to greater binding by the serum proteins and reduced performance in the presence of serum. Additionally, Chi/M-VLP exhibited significantly better transfection efficiency in the presence of serum than Lip/M-VLP and comparable transfection compared to MLV-A, particularly up to 30% serum (Figure 4), suggestive of possible improved *in vivo* performance and biodistribution. However, while additional elements such as PEGylation can be incorporated in the vector design [52], the current implementation of our hybrid vectors seems best suited to *ex vivo* transfection or non-vascular routes of gene therapy. The absence of the envelope protein of the retrovirus in our vector design may provide reduced immunogenicity without compromising the therapeutic gene delivery efficiency. Further work will be directed toward studying the biodistribution and delivery efficiency of the hybrid vectors *in vivo* through various routes of administration.

CONCLUSION

Hybrid vectors represent a promising new generation of efficient gene delivery agents. The elucidation of their intracellular trafficking process within the cell provides further evidence that viruses or virus-like particles can have significantly different interactions with cells depending on their primary internalization mechanism. This line of thought has been the subject of previous work [53,54] and we further expound the concept by including synthetic components with the retrovirus-like particle, M-VLP. Our design shows that the hybrid vector efficiency and trafficking kinetics can be significantly modulated via changes in the type and composition of synthetic agents used to complex with the M-VLP. Chi/M-VLPs were slower than Lip/M-VLPs in gene delivery due to the delayed dissociation of chitosan (>32 h) whereas the synthetic lipids dissociated from the M-VLPs much earlier during the

trafficking process (<8 h). Both forms of hybrid vectors relied on different processes of endocytosis. CME, CavME and MP could all provide successful gene delivery. Lip/M-VLP were also able to initiate uptake via membrane fusion but failed at gene delivery in doing so. Caveolar pathways had a significant role in the late stage trafficking of Chi/M-VLP, irrespective of the pH of chitosan used. However, Chi/M-VLP when synthesized using chitosan at pH 3 was also able to effectively use the endosomal release mechanism typically part of CME resulting in high transfection efficiency. The lipid composition of Lip/M-VLP significantly affected the optimal uptake and trafficking pathways for gene delivery wherein cholesterol-rich Lip/M-VLP preferred CavME while DOPE-rich Lip/M-VLP preferred CME for optimal transfections. Lip_{587}/M-VLP was able to use multiple pathways for transfections, possibly a reason for being the most optimal composition as reported earlier [5].

Supplementary Material

Refer to Web version on PubMed Central for supplementary material.

Acknowledgments

References

1. Verma IM, Somia N. Gene therapy -- promises, problems and prospects. Nature. 1997; 389:239–42. [PubMed: 9305836]

2. Ramsey JD, Vu HN, Pack DW. A top-down approach for construction of hybrid polymer-virus gene delivery vectors. J Control Release. 2010; 144:39–45. [PubMed: 20117154]

3. Drake DM, Keswani RK, Pack DW. Effect of Serum on Transfection by Polyethylenimine/Virus-Like Particle Hybrid Gene Delivery Vectors. Pharm Res. 2010; 27:2457–2465. [PubMed: 20730559]

4. Keswani R, Su K, Pack DW. Efficient In Vitro Gene Delivery by Hybrid Biopolymer/Virus Nanobiovectors. J Control Release. 2014; 192:40–46. [PubMed: 25009978]

5. Keswani RK, Pozdol IM, Pack DW. Design of hybrid lipid/retroviral-like particle gene delivery vectors. Mol Pharm. 2013; 10:1725–35. [PubMed: 23485145]

6. Khalil IA, Kogure K, Akita H, Harashima H. Uptake Pathways and Subsequent Intracellular Trafficking in Nonviral Gene Delivery. Pharmacol Rev. 2006; 58:32–45. [PubMed: 16507881]

7. Patil SD, Rhodes DG, Burgess DJ. DNA-based therapeutics and DNA delivery systems: a comprehensive review. AAPS J. 2005; 7:E61–77. [PubMed: 16146351]

8. Anderson JL, Hope TJ. Intracellular trafficking of retroviral vectors: obstacles and advances. Gene Ther. 2005; 12:1667–78. [PubMed: 16292352]

9. Pichon C, Billiet L, Midoux P. Chemical vectors for gene delivery: uptake and intracellular trafficking. Curr Opin Biotechnol. 2010; 21:640–645. [PubMed: 20674331]

10. Vaughan EE, DeGiulio JV, Dean Da. Intracellular trafficking of plasmids for gene therapy: mechanisms of cytoplasmic movement and nuclear import. Gene Ther. 2006; 6:671–81.

11. Doherty GJ, McMahon HT. Mechanisms of endocytosis. Biochem. 2009; 78:857–902.

12. Mercer J, Helenius A. Virus entry by macropinocytosis. Nat Cell Biol. 2009; 11:510–20. [PubMed: 19404330]

13. Rejman J, Bragonzi A, Conese M. Role of clathrin- and caveolae-mediated endocytosis in gene transfer mediated by lipo- and polyplexes. Mol Ther. 2005; 12:468–74. [PubMed: 15963763]

14. Rejman J, Oberle V, Zuhorn IS, Hoekstra D. Size-dependent internalization of particles via the pathways of clathrin- and caveolae-mediated endocytosis. Biochem J. 2004; 377:159–69. [PubMed: 14505488]

15. Parton RG, Simons K. The multiple faces of caveolae. Nat Rev Mol Cell Biol. 2007; 8:185–194. [PubMed: 17318224]

16. Nabi IR, Le PU. Caveolae/raft-dependent endocytosis. J Cell Biol. 2003; 161:673–7. [PubMed: 12771123]

17. Hashimoto, M.; Yang, Z.; Koya, Y.; Sato, T. Chitosan. In: Taira, K.; Kataoka, K.; Niidome, T., editors. Non-Viral Gene Ther. Springer; Tokyo: 2005. p. 63-74.

18. Rejman J, Conese M, Hoekstra D. Gene transfer by means of lipo- and polyplexes: role of clathrin and caveolae-mediated endocytosis. J Liposome Res. 2006; 16:237–47. [PubMed: 16952878]

19. Felgner PL, Gadek TR, Holm M, Roman R, Chan HW, Wenz M, et al. Lipofection: a highly efficient, lipid-mediated DNA-transfection procedure. Proc Natl Acad Sci. 1987; 84:7413–7. [PubMed: 2823261]

20. Simões S, Slepushkin V, Düzgünes N, Pedroso de Lima MC. On the mechanisms of internalization and intracellular delivery mediated by pH-sensitive liposomes. Biochim Biophys Acta. 2001; 1515:23–37. [PubMed: 11597349]

21. Karanth H, Murthy RSR. pH-sensitive liposomes--principle and application in cancer therapy. J Pharm Pharmacol. 2007; 59:469–83. [PubMed: 17430630]

22. Xu L, Anchordoquy TJ. Effect of Cholesterol Nanodomains on the Targeting of Lipid-Based Gene Delivery in Cultured Cells. Mol Pharm. 2010; 7:1311–1317. [PubMed: 20568694]

23. Ma PL, Buschmann MD, Winnik FM. One-step analysis of DNA/chitosan complexes by field-flow fractionation reveals particle size and free chitosan content. Biomacromolecules. 2010; 11:549–54. [PubMed: 20158194]

24. Ma O, Lavertu M, Sun J, Nguyen S, Buschmann MD, Winnik FM, et al. Precise derivatization of structurally distinct chitosans with rhodamine B isothiocyanate. Carbohydr Polym. 2008; 72:616–624.

25. Ivanov AI. Pharmacological inhibition of endocytic pathways: is it specific enough to be useful? Methods Mol Biol. 2008; 440:15–33. [PubMed: 18369934]

26. Sallusto BF, Cella M, Danieli C, Lanzavecchia A. Dendritic Cells Use Macropinocytosis and the Mannose Receptor to Concentrate Macromolecules in the Major Histocompatibility Complex Class II Compartment: Downregulation by Cytokines and Bacterial Products. J Exp Med. 1995; 182:389–400. [PubMed: 7629501]

27. Fumoto S, Nishi J, Ishii H, Wang X, Miyamoto H, Yoshikawa N, et al. Rac-Mediated Macropinocytosis Is a Critical Route for Naked Plasmid DNA Transfer in Mice. Mol Pharm. 2009:850–858.

28. Phonphok Y, Rosenthal KS. Stabilization of clathrin coated vesicles by amantadine, tromantadine and other hydrophobic amines. FEBS. 1991; 281:188–190.

29. Fredericksen BL, Wei BL, Yao J, Luo T, Garcia JV. Inhibition of endosomal/lysosomal degradation increases the infectivity of human immunodeficiency virus. J Virol. 2002; 76:11440–6. [PubMed: 12388705]

30. Sofer A, Futerman A. Cationic Amphiphilic Drugs Inhibit the Internalization of Cholera Toxin to the Golgi Apparatus and the Subsequent Elevation of Cyclic AMP. J Biol Chem. 1995; 270:12117–122. [PubMed: 7744860]

31. Aoki T, Nomura R, Fujimoto T. Tyrosine phosphorylation of caveolin-1 in the endothelium. Exp Cell Res. 1999; 253:629–36. [PubMed: 10585286]

32. Akinc A, Thomas M, Klibanov AM, Langer R. Exploring polyethylenimine-mediated DNA transfection and the proton sponge hypothesis. J Gene Med. 2005; 7:657–63. [PubMed: 15543529]

33. Kichler A, Leborgne C, Coeytaux E, Danos O. Polyethylenimine-mediated gene delivery: a mechanistic study. J Gene Med. 2001; 3:135–44. [PubMed: 11318112]

34. Goddette DW, Frieden C. Actin Polymerization: Mechanism of action of Cytochalasin D. J Biol Chem. 1986; 261:15974–15980. [PubMed: 3023337]

35. Parton RG, Joggerst B, Simons K. Regulated internalization of caveolae. J Cell Biol. 1994; 127:1199–215. [PubMed: 7962085]

36. Balzarini J, Herdewijn P, De Clercq E. Differential Patterns of Intracellular Metabolism of 2′,3′-didehydro-2′,3′-dideoxythymidine and 3′-Azido-2′,3′-dideoxythymidine, 2 potent Anti-Human Immunodeficiency Virus Compounds. J Biol Chem. 1989; 264:6127–6133. [PubMed: 2539371]

37. Beer C, Andersen DS, Rojek A, Pedersen L. Caveola-Dependent Endocytic Entry of Amphotropic Murine Leukemia Virus. J Virol. 2005; 79:10776–10787. [PubMed: 16051869]

38. Beer C, Pedersen L, Wirth M. Amphotropic murine leukaemia virus envelope protein is associated with cholesterol-rich microdomains. Virol J. 2005; 2:36. [PubMed: 15840168]

39. Zhang Y, Anchordoquy TJ. The role of lipid charge density in the serum stability of cationic lipid/DNA complexes. Biochim Biophys Acta. 2004; 1663:143–57. [PubMed: 15157617]

40. Hernández-Caselles T, Villalaín J, Gómez-Fernández JC. Influence of liposome charge and composition on their interaction with human blood serum proteins. Mol Cell Biochem. 1993; 120:119–26. [PubMed: 8487752]

41. García L, Buñuales M, Düzgüne N, Tros de Ilarduya C, Bun M, De Ilarduya CT. Serum-resistant lipopolyplexes for gene delivery to liver tumour cells. Eur J Pharm Biopharm. 2007; 67:58–66. [PubMed: 17321729]

42. Duarte S, Faneca H, de Lima MCP. Non-covalent association of folate to lipoplexes: a promising strategy to improve gene delivery in the presence of serum. J Control Release. 2011; 149:264–72. [PubMed: 21044650]

43. Roberts R, Al-Jamal WT, Whelband M, Thomas P, Jefferson M, van den Bossche J, et al. Autophagy and formation of tubulovesicular autophagosomes provide a barrier against nonviral gene delivery. Autophagy. 2013; 9:667–82. [PubMed: 23422759]

44. Chan C, Ewert KK, Majzoub RN, Hwu Y, Liang KS, Leal C, et al. Optimizing cationic and neutral lipids for efficient gene delivery at high serum content. J Gene Med. 2014; 16:84–96. [PubMed: 24753287]

45. Xu L, Anchordoquy T. Drug Delivery Trends in Clinical Trials and Translational Medicine: Challenges and Opportunities in the Delivery of Nucleic Acid-Based Therapeutics. J Pharm Sci. 2010; 100:38–52. [PubMed: 20575003]

46. Balazs DA, Godbey WT. Liposomes for use in gene delivery. J Drug Deliv. 2011; 2011:326497. [PubMed: 21490748]

47. Peng SF, Tseng MT, Ho YC, Wei MC, Liao ZX, Sung HW. Mechanisms of cellular uptake and intracellular trafficking with chitosan/DNA/poly(γ-glutamic acid) complexes as a gene delivery vector. Biomaterials. 2011; 32:239–48. [PubMed: 20864162]

48. Thibault M, Nimesh S, Lavertu M, Buschmann MD. Intracellular Trafficking and Decondensation Kinetics of Chitosan-pDNA Polyplexes. Gene Ther. 2010; 18:1787–1795.

49. Douglas KL, Piccirillo Ca, Tabrizian M. Cell line-dependent internalization pathways and intracellular trafficking determine transfection efficiency of nanoparticle vectors. Eur J Pharm Biopharm. 2008; 68:676–87. [PubMed: 17945472]

50. Wu Y, Ho Y, Mao Y, Wang X, Yu B, Leong KW, et al. Uptake and Intracellular Fate of Multifunctional Nanoparticles: A Comparison between Lipoplexes and Polyplexes via Quantum Dot Mediated Forster Resonance Energy Transfer. Mol Pharm. 2011; 8:1662–1668. [PubMed: 21740056]

51. Mundy DI, Li WP, Luby-Phelps K, Anderson RGW. Caveolin targeting to late endosome/lysosomal membranes is induced by perturbations of lysosomal pH and cholesterol content. Mol Biol Cell. 2012; 23:864–80. [PubMed: 22238363]

52. Mao H, Roy K, Troung-le VL, Janes KA, Lin KY, Wang Y, et al. Chitosan-DNA nanoparticles as gene carriers: synthesis, characterization and transfection efficiency. J Control Release. 2001; 70:399–421. [PubMed: 11182210]

53. Emi N, Friedmann T, Yee JK. Pseudotype formation of murine leukemia virus with the G protein of vesicular stomatitis virus. J Virol. 1991; 65:1202–7. [PubMed: 1847450]

54. Burns JC, Friedmann T, Driever W, Burrascano M, Yee JK. Vesicular stomatitis virus G glycoprotein pseudotyped retroviral vectors: concentration to very high titer and efficient gene

transfer into mammalian and nonmammalian cells. Proc Natl Acad Sci. 1993; 90:8033–7. [PubMed: 8396259]

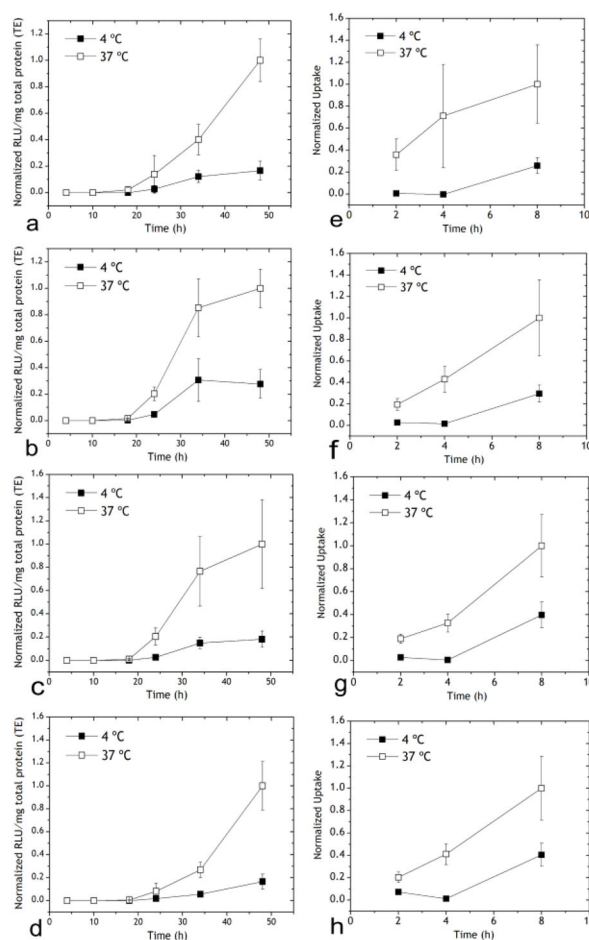**Figure 1.**
Transfection of HEK293 cells mediated by Chi/M-VLP at (a) 2 μg/10^9 M-VLPs, (b) 4 μg/10^9 M-VLPs, (c) 7 μg/10^9 M-VLPs, (d) 10 μg/10^9 M-VLPs. Cells were incubated with hybrid vectors at 4 C or 37 C as indicated for 4 h following which the vectors were removed and replaced with fresh media, and the cells were incubated at 37 C for the remainder of the experiment. Luciferase activity (RLU/mg total protein) was normalized to the corresponding values 48 h post-transfection at 37 °C. Cellular uptake of Chi/M-VLP at (e) 2 μg/10^9 M-VLPs, (f) 4 μg/10^9 M-VLPs, (g) 7 μg/10^9 M-VLPs, (h) 10 μg/10^9 M-VLPs at 4 °C and 37 °C for 4 h as with the transfections. Uptake of Chi/M-VLP was normalized to the corresponding values 8 h post-transfection at 37 °C. Error bars represent SD, n=3.
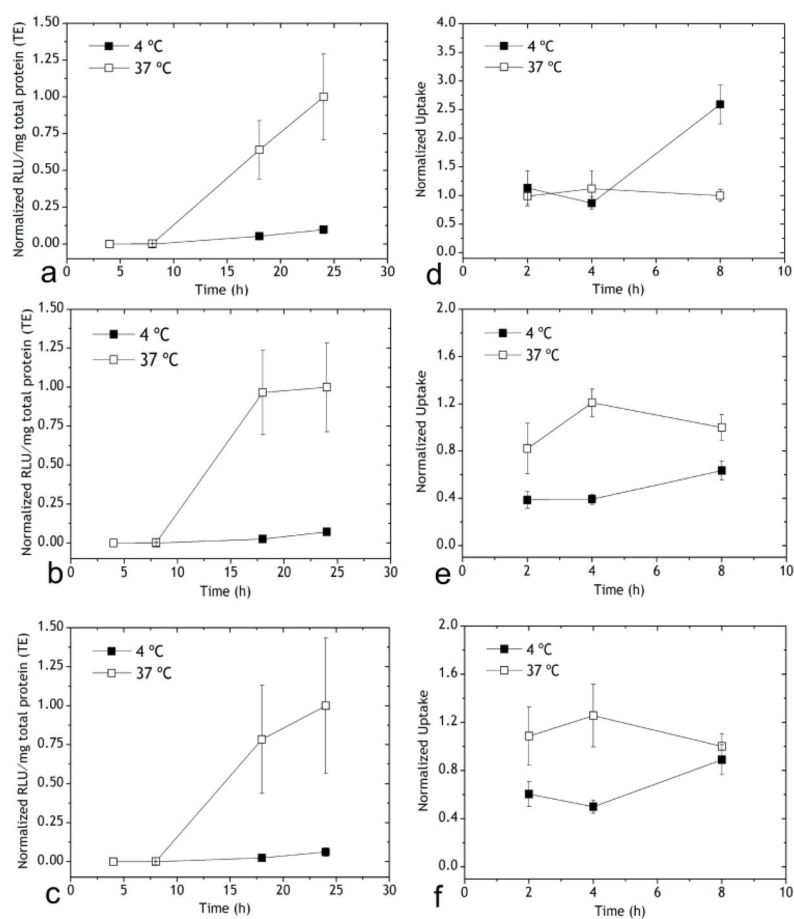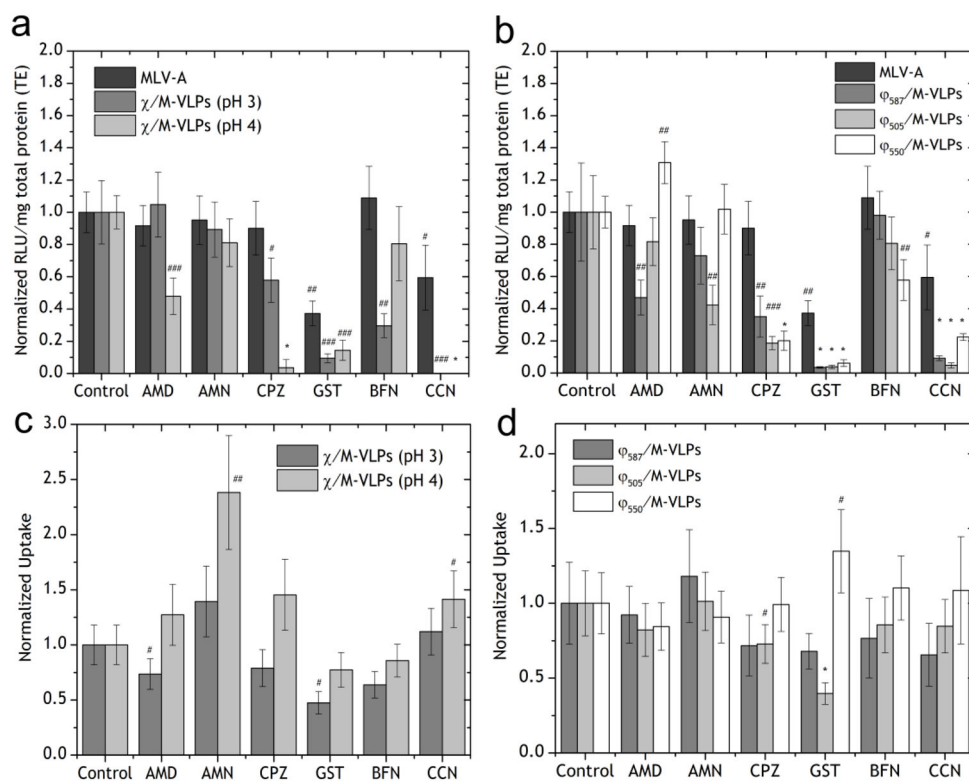
Figure 2.
Transfection of Lip/M-VLP at (a) 10 μg/10^9 M-VLPs Lip$_{587}$/M-VLP, (b) 10 μg/10^9 M-VLPs Lip$_{505}$/M-VLP, (c) 10 μg/10^9 M-VLPs Lip$_{550}$/M-VLP at 4 °C and 37 °C. Cells were incubated with hybrid vectors at 4 °C or 37 °C for 4 h after which the vectors were removed and replaced with fresh media, and the cells were incubated at 37 °C for the remainder of the experiment. Luciferase activity (RLU/mg total protein) was normalized to the corresponding values 48 h post-transfection at 37 °C. Cellular uptake of Lip/M-VLP at (d) 10 μg/10^9 M-VLPs Lip$_{587}$/M-VLP, (e) 10 μg/10^9 M-VLPs Lip$_{505}$/M-VLP and (f) 10 μg/10^9 M-VLPs Lip$_{550}$/M-VLP at 4 °C and 37 °C for 4 h as with the transfections. Uptake of Chi/M-VLP was normalized to the corresponding values 8 h post-transfection at 37 °C. Error bars represent SD, n=3.

Figure 3.
Transfection of HEK293 cells by (a) MLV-A and Chi/M-VLP (pH 3 and pH 4, 5 μg/10^9 M-VLPs) and (b) MLV-A and Lip$_{587}$/M-VLP, Lip$_{505}$/M-VLP and Lip$_{550}$/M-VLP (10 μg/10^9 M-VLPs) in the presence of drug inhibitors. Luciferase activity in treated cells was normalized to expression in untreated cells. Cellular uptake of (c) Chi/M-VLP (pH 3 and pH 4, 5 μg/10^9 M-VLPs) and (d) Lip$_{587}$/M-VLP$_{DiD}$, Lip$_{505}$/M-VLP$_{DiD}$ and Lip$_{550}$/M-VLP$_{DiD}$ (10 μg/10^9 M-VLPs) in the presence of drug inhibitors normalized to corresponding values in untreated cells. Error bars represent SD, n=3 (# - $p < 0.05$, ## - $p < 0.02$, ### - $p < 0.002$ and * - $p < 0.0001$).
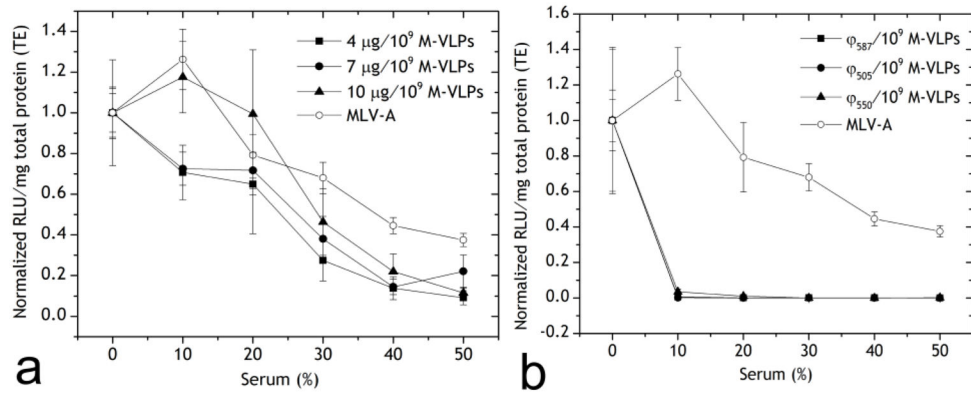
Figure 4.
Transfection of HEK293 cells by (a) Chi/M-VLP and MLV-A, and (b) Lip_{587}/M-VLP, Lip_{505}/M-VLP, Lip_{550}/M-VLP (10 μg/10^9 M-VLPs) and MLV-A in the presence of various concentrations of serum. Luciferase activity was normalized to the corresponding values in 0% serum. Error bars represent SD, n=3.
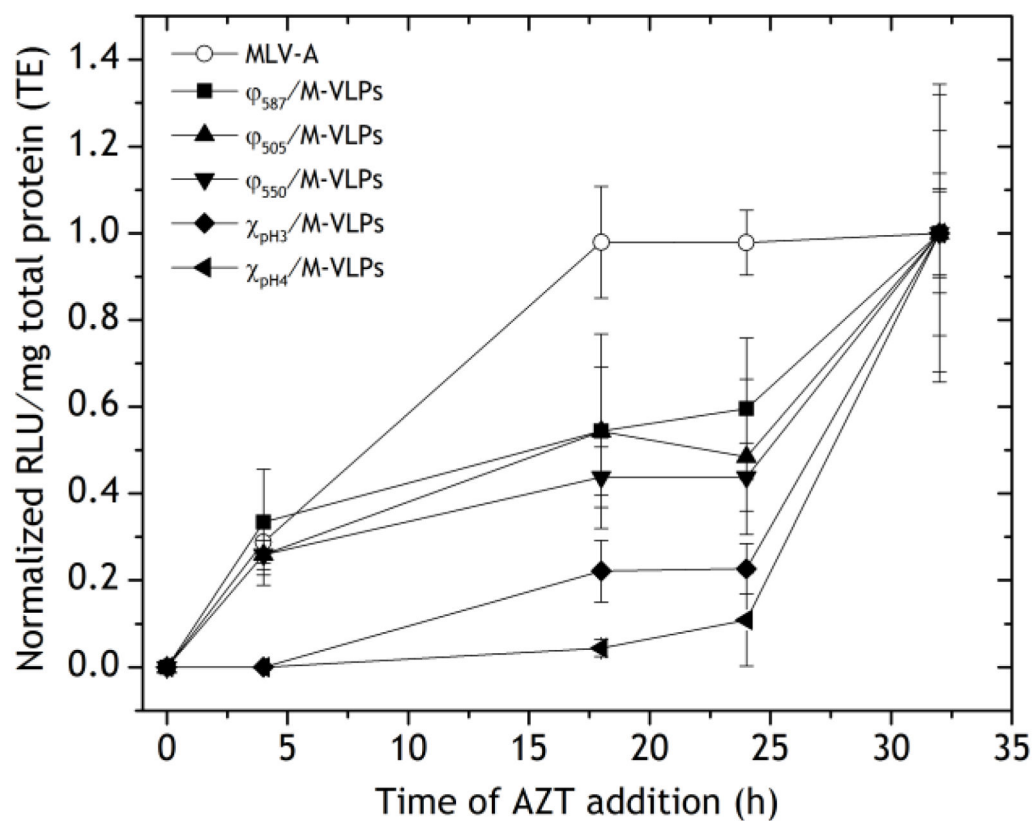
Figure 5.
Transfection of HEK293 cells by Chi/M-VLP (pH 3 and pH 4, 5 µg/10^9 M-VLPs), Lip$_{587}$/M-VLP, Lip$_{505}$/M-VLP, Lip$_{550}$/M-VLP (10 µg/10^9 M-VLPs) and MLV-A in the presence of AZT added 0, 4, 18, 24 and 32 h post-transfection. Luciferase expression was normalized to the corresponding values when treated with AZT 32 h post-transfection. Error bars represent SD, n=3.
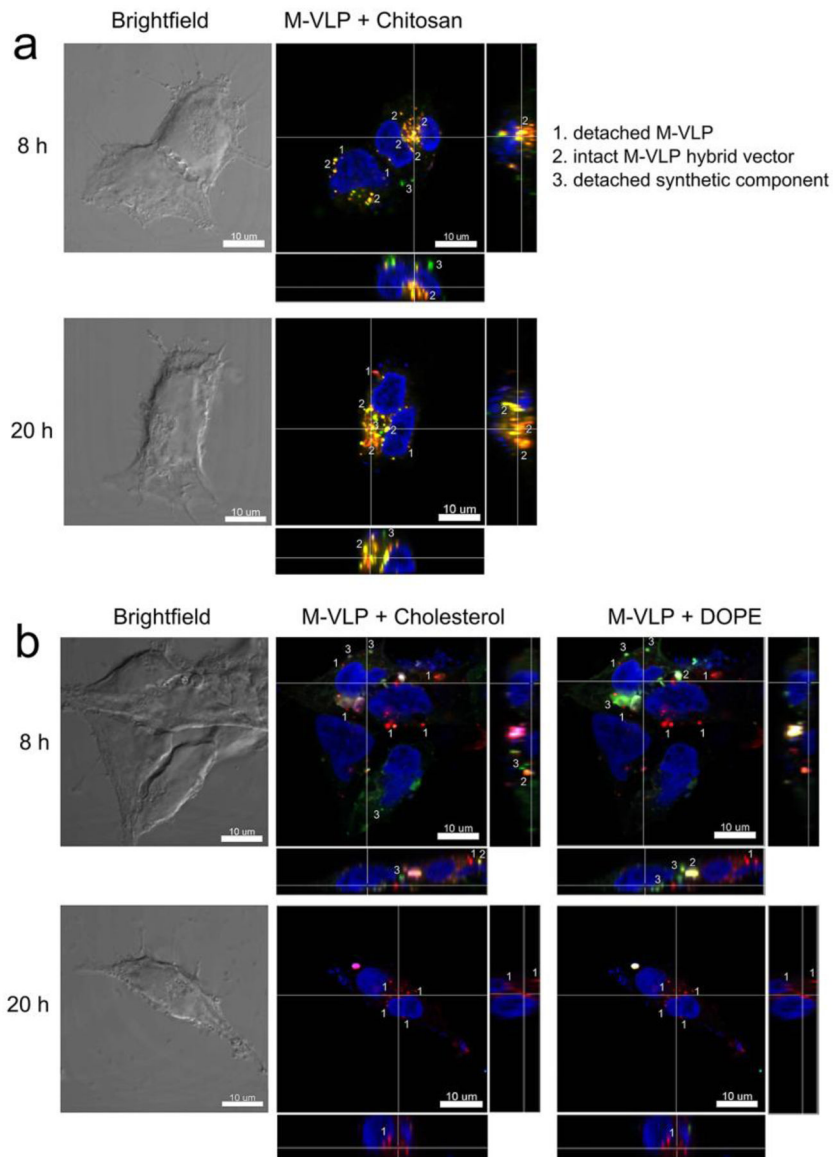
Figure 6.
Confocal fluorescence microscopy of HEK293 cells transfected with (a) Chi/M-VLP (5 μg/10^9 M-VLPs) or (b) Lip$_{587}$/M-VLP (10 μg/10^9 M-VLPs) at 8 and 20 h post-transfection. Fluorescent labels were DiD (M-VLPs, *red*), RITC (chitosan, *green*), Rhod-B (DOPE, *green*) and NBD-6-cholesterol (*green*). Cell nucleus was counterstained with DAPI (*blue*). Scale bar = 10 μm.

Table 1

Mechanism of action and optimal concentration of drug inhibitors used in this study.

Drug	Effect	Optimal Concentration
Amiloride (AMD)	Inhibition of Na^+/H^+ exchange[26,27] (MP)	50 μg/ml
Amantadine (AMN)	Stabilization of clathrin-coated vesicles[28], increases endosomal pH [29] (CME)	100 μg/ml
Chlorpromazine (CPZ)	Disrupts assembly and disassembly of clathrin from coated pits[30] (CME)	20 μM
Genistein (GST)	Inhibits tyrosine phosphorylation preventing caveolae formation[31] (CavME)	20 μg/ml
Bafilomycin A1 (BFN)	Prevents re-acidification of synaptic vesicles inhibiting release of endosomal cargo[32,33] (CME)	5 nM
Cytochalasin D (CCN)	Inhibits actin polymerization and caveolae formation [34,35] (CavMe, Fusion)	10 μM
Azidothymidine (AZT)	Inhibits reverse transcription[36]	20 μM